COMMUNICATIONS IN COMPUTATIONAL PHYSICS
Vol. **1**, No. 6, pp. 1043-1055

Commun. Comput. Phys.
December 2006

Analysis and Numerical Solution of Transient Electromagnetic Scattering from Overfilled Cavities

Junqi Huang and Aihua Wood*

Air Force Institute of Technology, 2950 Hobson Way, AFIT/ENC, WPAFB, OH, 45433-7765, USA.

Received 12 December 2005; Accepted (in revised version) 8 May 2006

Abstract. A hybrid finite element (FEM) and Fourier transform method is implemented to analyze the time domain scattering of a plane wave incident on a 2-D overfilled cavity embedded in the infinite ground plane. The algorithm first removes the time variable by Fourier transform, through which a frequency domain problem is obtained. An artificial boundary condition is then introduced on a hemisphere enclosing the cavity that couples the fields from the infinite exterior domain to those inside. The exterior problem is solved analytically via Fourier series solutions, while the interior region is solved using finite element method. In the end, the image functions in frequency domain are numerically inverted into the time domain. The perfect link over the artificial boundary between the FEM approximation in the interior and analytical solution in the exterior indicates the reliability of the method. A convergence analysis is also performed.

Key words: Time domain; overfilled cavity; scattering; Fourier transform; finite element method.

1 Introduction

Transient Maxwell's equations for electromagnetic scattering problems have been studied extensively both in theory and computation. One of the important advantages of these equations over their time-harmonic counterparts is that one can obtain the scattering properties such as radar cross sections (RCS) of scatterers for a wide range of frequencies with a single analysis by an application of Fourier transform. Integral equation methods with retarded potentials have been analyzed and successfully implemented for both perfectly conducting and homogeneous dielectric bodies (See, for example, [1] and references

*Correspondence to: Aihua Wood, Air Force Institute of Technology, 2950 Hobson Way, AFIT/ENC, WPAFB, OH, 45433-7765, USA. Email: Aihua.Wood@afit.edu

therein). For the more complex heterogeneous scattering bodies, variational methods are easier to be formulated and simulated. Among the scattering problems, of particular interest is the study of electromagnetic scattering from cavities and the calculation of their RCS. This is because cavity RCS often dominates a target's overall RCS and is computationally challenging. One of the main difficulties in numerically approximating solutions involving cavities is the appearance of spurious modes caused by interior resonances. A variety of techniques have been developed to simulate the scattering by cavities. They include high and low frequency methods [5, 8, 12],the method of moments [19, 21], the time domain finite difference method [6], and hybrid methods [9–11, 13, 14]. Mathematical treatment of scattering problems involving cavities can be found in [2–4, 16]. It's a common assumption that the cavity opening coincides with the aperture on an infinite ground plane, and hence simplifying the modelling of the exterior (to the cavity) domain. This severely limits the application of these methods since many cavity openings are not planar. In [18], a mathematical model characterizing the scattering by over-filled cavities was developed and proved well-posed. In particular, the method decomposes the entire infinite solution domain to two sub-domains: the infinite upper half plane over the perfect electrically conducting (PEC) ground plane exterior to the hemisphere enclosing the cavity aperture, and the cavity plus the hemisphere region. The problem is solved exactly in the infinite sub-domain, while the other is solved using finite elements. The two regions are coupled over the hemisphere via the introduction of a boundary operator exploiting the field continuity over material interfaces.

Other methods designed to numerically determine the fields scattered by obstables/cavities which give rise to infinite computational domains include absorbing boundary conditions (ABC), perfectly matched layer (PML), and transparent boundary conditions (for a survey of non-reflecting boundary conditions see [7]). In [15], transient Maxwell's equations for the electric field are first discretized in time by Newmark's time-stepping scheme. Then, at each time step a nonlocal boundary condition is imposed on the cavity opening, i.e. the interface between the cavity and the upper half space, to enable the scattering problem to be restricted to the cavity itself. A variational formulation of the problem is derived and shown to possess a unique weak solution at each time step. In [17], the variational problem is fully discretized by first-order edge elements of the first type. There, approximating problems are shown to admit unique solutions and they converge to the exact solutions provided the cavity is characterized by a regular electric permittivity ε.

In this paper, we first apply Fourier transform with respect to time t to the governing wave equation, resulting in a Helmholtz equation in the frequency domain. We then analytically solve the exterior problem via Fourier transform, getting an analytical formula which is incorporated in the boundary condition of the variational problem defined in the interior domain. The interior problem is subsequently solved via the finite element method. At last, the image functions in the frequency domain are numerically inverted into the real time domain by employing the cubic spline interpolation. We also investigate the convergence property of the method.

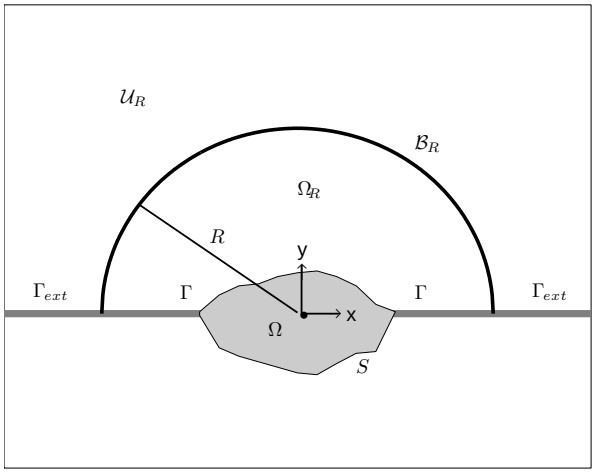

Figure 1: Cavity setting.

2 Problem setting

Let $\Omega \subset \mathbb{R}^2$ be the cross section of a z-invariant cavity (or trough) in the infinite ground plane such that its fillings of relative permittivity $\varepsilon_r \geq 1$ protrudes above the ground plane. Let $(\boldsymbol{E}^i, \boldsymbol{H}^i)$ be an electromagnetic wave incident on the cavity to generate the scattered field $(\boldsymbol{E}^s, \boldsymbol{H}^s)$. The scattering problem is to find $(\boldsymbol{E}^s, \boldsymbol{H}^s)$.

In the rest of the paper, we will denote Ω as the sub domain occupied by the cavity, Ω_R the sub domain above the cavity and below the artificial boundary $\mathcal{B}_R$ consists of a semicircle with radius R, $\mathcal{U}_R$ the homogenous region above $\mathcal{B}_R$, Γ and Γ_{ext} the ground plane respectively inside and outside $\mathcal{B}_R$, S the wall of the cavity. Details are depicted in Fig. 1. For the convenience, indicating $\mathcal{U} = \Omega_R \bigcup \mathcal{U}_R$ and $\Gamma_{tol} = \Gamma \bigcup \Gamma_{ext}$.

Due to the uniformity in the z-axis, the scattering problem can be decomposed into two fundamental polarizations: transverse magnetic (TM) and transverse electric (TE). Its solution then can be expressed as a linear combination of the solutions to TM and TE problems. In the TM polarization, the magnetic field $\boldsymbol{H}$ is transverse to the z-axis so that $\boldsymbol{E}$ and $\boldsymbol{H}$ are of the form

$$\boldsymbol{E} = (0, 0, E_z), \quad \boldsymbol{H} = (H_x, H_y, 0). \tag{2.1}$$

In this case, the nonzero component of the total field, also denoted as $\boldsymbol{E}$, satisfies the following equation

$$\text{(TM)} \begin{cases} -\Delta E_z + \varepsilon_r \dfrac{\partial^2 E_z}{\partial t^2} &= 0 \quad \text{in } \Omega \cup \mathcal{U} \times (0, \infty) \\ E_z &= 0 \quad \text{on } S \cup \Gamma_{tol} \times (0, \infty), \\ E_z|_{t=0} = E_0, & \dfrac{\partial E_z}{\partial t}|_{t=0} = E_{t,0}, \end{cases} \tag{2.2}$$

where ε_r is the relative electric permittivity, E_0 and $E_{t,0}$ are given initial conditions. The homogeneous region $\mathcal{U}$ above the protruding cavity is assumed to be air and hence, its permittivity is $\varepsilon_r = 1$. In $\mathcal{U}$, the total field can be decomposed as $E_z = E_z^i + E_z^r + E_z^s$ where E_z^i is the incident field, E_z^r the reflected field, and E_z^s the scattered field. The reflected field exists due to the presence of the infinite ground plane. The incident and reflected electric fields satisfy

$$E_z^i + E_z^r = 0 \quad \text{on } \Gamma_{tol} \subset \{(x,y) : y = 0\}. \tag{2.3}$$

The scattered field E_z^s solves the following equation

$$(\mathrm{TM}^s) \quad \begin{cases} -\Delta E_z^s + \dfrac{\partial^2 E_z^s}{\partial t^2} &= 0 \quad \text{in } \mathcal{U} \times (0,\infty), \\ E_z^s &= E_z - E_z^i - E_z^r \quad \text{on } \Gamma \times (0,\infty), \\ E_z^s &= 0 \quad \text{on } \Gamma_{tol} \times (0,\infty), \end{cases} \tag{2.4}$$

and satisfies the radiation condition at infinity, that is,

$$\lim_{r\to\infty} \sqrt{r} \left(\frac{\partial E_z^s}{\partial r} + \frac{\partial E_z^s}{\partial t} \right) = 0, \quad t > 0. \tag{2.5}$$

The components of $\boldsymbol{H}$ can be obtained in terms of E_z and its partial derivatives by using Maxwell's equations.

Similarly, in the TE polarization, the electric field $\boldsymbol{E}$ is transverse to the z-axis and hence,

$$\boldsymbol{E} = (E_x, E_y, 0), \quad \boldsymbol{H} = (0, 0, H_z). \tag{2.6}$$

The nonzero component of the total magnetic field, also denoted by $\boldsymbol{H}$, satisfies the following equation

$$(\mathrm{TE}) \quad \begin{cases} -\nabla \cdot \left(\dfrac{1}{\varepsilon_r} \nabla H_z \right) + \dfrac{\partial^2 H_z}{\partial t^2} &= 0 \quad \text{in } \Omega \cup \mathcal{U} \times (0,\infty), \\ \dfrac{\partial H_z}{\partial n} &= 0 \quad \text{on } S \cup \Gamma_{tol} \times (0,\infty), \\ H_z|_{t=0} = H_0, \qquad \dfrac{\partial H_z}{\partial t}|_{t=0} = H_{t,0}, \end{cases} \tag{2.7}$$

where H_0 and $H_{t,0}$ are given initial conditions. In U_R, the total magnetic field can be decomposed into $H_z = H_z^i + H_z^r + H_z^s$ where

$$\frac{\partial H_z^i}{\partial y} + \frac{\partial H_z^s}{\partial y} = 0 \quad \text{on } \{(x,y) : y = 0\}. \tag{2.8}$$

The scattered field solves

$$(\mathrm{TE}^s) \quad \begin{cases} -\Delta H_z^s + \dfrac{\partial^2 H_z^s}{\partial t^2} &= 0 \quad \text{in } \mathcal{U} \times (0,\infty), \\ \dfrac{\partial H_z^s}{\partial n} &= 0 \quad \text{on } \Gamma_{tol}, \\ \dfrac{\partial H_z^s}{\partial n} &= \dfrac{1}{\varepsilon_r} \dfrac{\partial H_z}{\partial n} - \dfrac{\partial H_z^i}{\partial n} - \dfrac{\partial H_z^r}{\partial n} \quad \text{on } \Gamma \times (0,\infty), \end{cases} \tag{2.9}$$

where $\partial/\partial n$ is the normal derivative on Γ. The scattered magnetic field also satisfies the same radiation condition defined in (2.5). The components of $\boldsymbol{E}$ can be obtained in terms of H_z and its partial derivatives by using Maxwell's equations.

3 TM polarization

For convenience, we denote u^i as the incident field E_z^i, u^r the reflected field E_z^r, u the total field E_z, and u^s the scattered field E_z^s. The scattered field u^s satisfies the following exterior problem:

$$\begin{aligned} -\Delta u^s + \frac{\partial^2 u^s}{\partial t^2} &= 0 \quad \text{in } \mathcal{U}_R, t > 0, && (3.1)\\ u^s &= u_R^s \quad \text{on } \mathcal{B}_R, t > 0, && (3.2)\\ u^s &= 0 \quad \text{on } \Gamma_{ext}, t > 0, && (3.3)\\ u^s = \partial u^s/\partial t &= 0 \quad \text{at } t = 0, && (3.4) \end{aligned}$$

and the radiation condition:

$$\lim_{r\to\infty} \sqrt{r}\left(\frac{\partial u^s}{\partial r} + \frac{\partial u^s}{\partial t}\right) = 0., t > 0 \tag{3.5}$$

where the time is scaled by the light velocity c, (t/c). In addition, as shown in Figure 1, $\mathcal{U}_R$ indicates exterior domain of artificial boundary $\mathcal{B}_R$. With Fourier transform $\{t \to \omega, u \to U\}$, Equation (3.1) subject to the initial condition (3.4) becomes

$$\Delta U^s + \omega^2 U^s = 0 \quad \text{in } \mathcal{U}_R, \tag{3.6}$$

and with the radiation condition

$$\lim_{r\to\infty} \sqrt{r}\left(\frac{\partial U^s}{\partial r} + i\omega U^s\right) = 0, \tag{3.7}$$

where, U^s is the image of u^s, ω the Fourier transform parameter or the frequency.

In polar coordinates, the Helmholtz Equation (3.6) becomes

$$\frac{\partial^2 U^s}{\partial r^2} + \frac{1}{r}\frac{\partial U^s}{\partial r} + \frac{1}{r^2}\frac{\partial^2 U^s}{\partial \theta^2} + \omega^2 U^s = 0. \tag{3.8}$$

The solution of equation (3.8) subject to the boundary condition (3.2)-(3.3) and radiation condition (3.7) is

$$U^s = \frac{2}{\pi}\sum_{n=1}^{\infty} \frac{H_n^{(k)}(\omega r)}{H_n^{(k)}(\omega R)} \sin(n\theta) \int_0^{\pi} U_R^s(\varphi)\sin(n\varphi)d\varphi, \tag{3.9}$$

where $H_n^{(k)}(\cdot)$ is the Hankel function with $k=1$ as $\omega<0$ and $k=2$ as $\omega\geq 0$, U_R^s indicates U^s along $\mathcal{B}_R$. Define the boundary operator

$$\overline{T}: H^{1/2}(\mathcal{B}_{\mathcal{R}}) \to H^{-1/2}(\mathcal{B}_{\mathcal{R}})$$

as

$$\overline{T}(y) = \frac{2}{\pi}\sum_{n=1}^{\infty}\left(\frac{\omega H_n^{(k)'}(\omega r)}{H_n^{(k)}(\omega R)}\int_0^{\pi} y\,\sin(n\varphi)d\varphi\right)\sin(n\theta). \tag{3.10}$$

With this operator, we have the following interior problem for the total field in Fourier domain:

$$\begin{aligned} \Delta U\omega^2\epsilon_r U &= 0 \quad \text{in } \Omega_R\bigcup\Omega, &(3.11)\\ \partial U/\partial r - T(U) &= \bar{g} \quad \text{on } \mathcal{B}_R, &(3.12)\\ U &= 0 \quad \text{on } \Gamma\cup S, &(3.13)\end{aligned}$$

where $\bar{g}=\partial(U^i+U^r)/\partial r - T(U^i+U^r)$, U^i and U^r are the incident and reflected fields in the Fourier domain respectively.

With *pdetool* under GUI environment of Matlab, Equation (3.11) is classified as elliptic equation, and (3.12), the generalized Neumann boundary condition, can be discretized accordingly. We have the stiffness matrix

$$K_{i,j} = \int_{\Omega_R}\nabla\phi_j\cdot\nabla\phi_i dxdy, \tag{3.14}$$

the mass matrix

$$M_{i,j} = \omega^2\int_{\Omega_R}\epsilon_r\phi_j\phi_i dxdy, \tag{3.15}$$

and the boundary matrix

$$G_i = R\int_0^{\pi}\bar{g}\phi_i d\theta, \tag{3.16}$$

which can all be generated automatically. Here, ϕ_i is the basis function. Contribution from the non-standard (artificial) boundary condition

$$Q_{i,j} = -R\int_0^{\pi} T(\phi_j)\phi_i d\theta \tag{3.17}$$

needs to be implemented manually. Let

$$u = \sum_{j=1}^{N_p} u_j\,\phi_j, \tag{3.18}$$

where N_p is the number of nodes. Substituting the above expression in (3.17) and simplifying gives

$$Q_{i,:} = -\frac{2R}{\pi}\sum_{n=1}^{\infty}\frac{\omega H_n^{(k)'}(\omega R)}{H_n^{(k)}(\omega R)}\beta_{n,i}\sum_{j=1}^{B}\beta_{n,j}, \tag{3.19}$$

where

$$\beta_{n,i} = \frac{1}{n^2}\left(\frac{\sin(n\theta_i)-\sin(n\theta_{i-})}{\theta_i-\theta_{i-}} - \frac{\sin(n\theta_{i+})-\sin(n\theta_i)}{\theta_{i+}-\theta_i}\right)$$

and θ_i is the central angle of node i located on $\mathcal{B}_R$; θ_{i-} and θ_{i+} are the central angles of left and right neighbors of node i, B is the number of node on the artificial boundary.

With expressions (3.14)-(3.16) and (3.19), we obtain the following discrete problem:

$$\sum_{j=1}^{N_p}(K_{i,j}+M_{i,j}+Q_{i,j})U_j = G_i, \quad 1\le i\le N_p. \tag{3.20}$$

4 TE polarization

In this case, the scattered field u^s satisfies the following exterior problem:

$$\begin{aligned}
-\Delta u^s + \frac{\partial^2 u^s}{\partial t^2} &= 0 \quad \text{in } \mathcal{U}_R, t>0, &(4.1)\\
u^s &= u_R^s \quad \text{on } \mathcal{B}_R, t>0, &(4.2)\\
\partial u^s/\partial n &= 0 \quad \text{on } \Gamma_{ext}, t>0, &(4.3)\\
u^s = \partial u^s/\partial t &= 0 \quad \text{at } t=0, &(4.4)
\end{aligned}$$

and the radiation condition (3.5). The solution in the Fourier domain is

$$U^s = \frac{2}{\pi}\sum_{n=0}^{\infty}\frac{\delta_n H_n^{(k)}(\omega r)}{H_n^{(k)}(\omega R)}\cos(n\theta)\int_0^{\pi}U_R^s(\varphi)\cos(n\varphi)d\varphi, \tag{4.5}$$

where δ_n is defined as $1/2$ for $n=0$ and 1 for $n>0$. As in the TM case, we define the boundary operator:

$$S(y) = \frac{2}{\pi}\sum_{n=0}^{\infty}\frac{\omega H_n^{(k)'}(\omega R)}{H_n^{(k)}(\omega R)}\cos(n\theta)\int_0^{\pi} y\,\cos(n\varphi)d\varphi. \tag{4.6}$$

Then the total magnetic field in the Fourier domain defined in Ω_R satisfies:

$$\begin{aligned}
\nabla\cdot(\epsilon_r^{-1}\nabla U)+\omega^2 U &= 0 \quad \text{in } \Omega_R\bigcup\Omega, &(4.7)\\
\partial U/\partial r - S(U) &= \bar{g} \quad \text{on } \mathcal{B}_R, &(4.8)\\
\partial U/\partial n &= 0 \quad \text{on } \Gamma\cup S, &(4.9)
\end{aligned}$$

where $\bar{g} = \partial(U^i + U^r)/\partial r - S(U^i + U^r)$.

The same difference scheme can then be applied here to obtain the discrete system. Specifically, we have the stiffness matrix

$$K_{i,j} = \int_{\Omega_R} \epsilon_r^{-1} \nabla\phi_j \cdot \nabla\phi_i dxdy, \tag{4.10}$$

the mass matrix

$$M_{i,j} = \omega^2 \int_{\Omega_R} \phi_j \phi_i dxdy, \tag{4.11}$$

the boundary matrices

$$G_i = R\int_0^\pi \epsilon_r^{-1} g^{m+1}\phi_i d\theta, \qquad Q_{i,j} = -R\int_0^\pi \epsilon_r^{-1} S(\phi_j)\phi_i d\theta. \tag{4.12}$$

As before, $Q_{i,j}$ can be further written as:

$$Q_{i,:} = -\frac{2R}{\pi}\sum_{n=1}^{\infty} \frac{\delta_n \omega H_n^{(k)'}(\omega R)}{H_n^{(k)}(\omega R)} \frac{\beta_{n,i}}{(\varepsilon_r)_i} \sum_{j=1}^{B} \beta_{n,j}, \tag{4.13}$$

where

$$\beta_{n,i} = \frac{1}{n^2}\left(\frac{\cos(n\theta_i) - \cos(n\theta_{i-})}{\theta_i - \theta_{i-}} - \frac{\cos(n\theta_{i+}) - \cos(n\theta_i)}{\theta_{i+} - \theta_i}\right).$$

The discretized system for the TE case follows similarly.

5 Numerical experiment

We consider a composite cavity of a triangular shape below the ground plane and circular above filled with a dielectric material of relative electric permittivity $\epsilon_r = 4 - i$. The geometry and mesh of the cavity is shown in Fig. 2. A Fourier frequency spectra is obtained by numerically scanning the space of frequency at selected nodes as show in Figs. 3 and 4.

For the frequency sequence $(100 : 0.5 : 100)$, the linear system (3.20) can be easily solved by calling the build-in functions of *pdetool*. The image solution then can be inverted to time domain using the following formula:

$$u = \frac{1}{2\pi}\int_{-\infty}^{\infty} U e^{-i\omega t} d\omega. \tag{5.1}$$

A cubic spline interpolant is implemented for U and may be expressed as

$$U = \sum_{k=1}^{N_f} \left[a_k \chi^3 + b_k \chi^2 + c_k \chi + d_k\right], \tag{5.2}$$

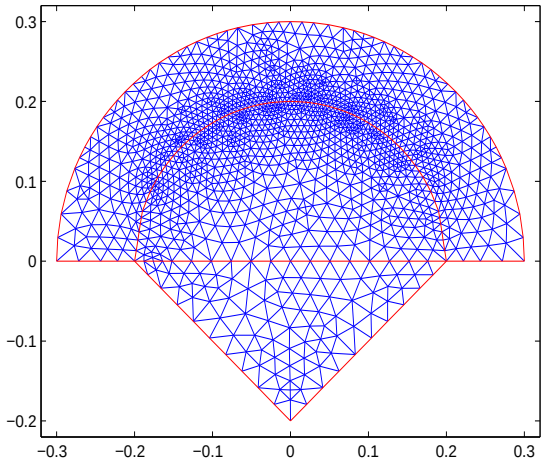

Figure 2: Cavity and mesh system, inner sector of the circle is the filled cavity, permittivity $\epsilon_r = 4 - i$.

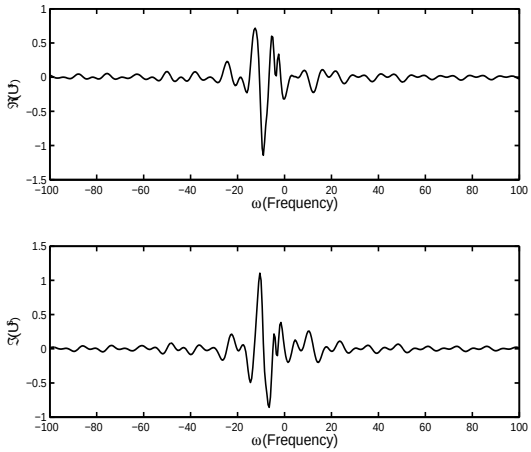

Figure 3: U^s versus ω for TM polarization, $r = 0.3m, \theta = \pi/2, k_0 = 2\pi, \theta^{inc} = \pi/2$.

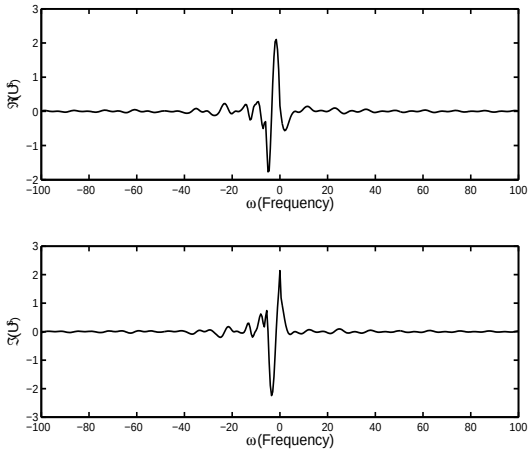

Figure 4: U^s versus ω for TE polarization, $r = 0.3m, \theta = \pi/2, k_0 = 2\pi, \theta^{inc} = \pi/2$.

where N_f is the number of interpolants, a_k, b_k, c_k and d_k are the spline coefficients related to ω_k and U_k, and $\chi = \omega - \omega_k$. Substituting (5.2) into (5.1) yields

$$u = \sum_{k=1}^{N_f} \int_{\omega_k}^{\omega_{k+1}} \left[a_k\chi^3 + b_k\chi^2 + c_k\chi + d_k\right] e^{-i\omega t} d\omega. \tag{5.3}$$

Each integration term in Equation (5.3) can be derived analytically. The time domain field solution can then be obtained by evaluating Equation (5.3) at selected notes in the mesh system.

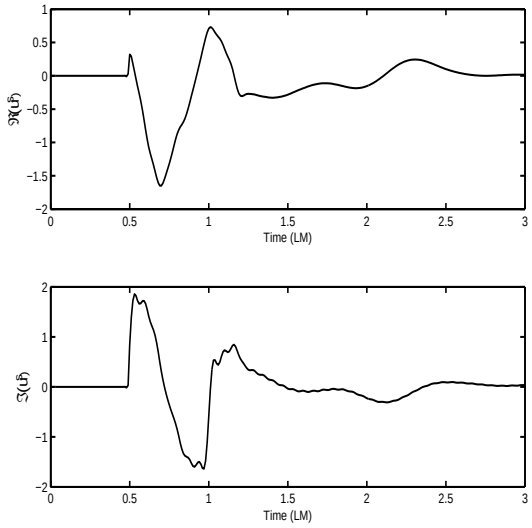

Figure 5: Change history of scattering field for TM polarization at $r = 0.3m, \theta = \pi/2$ with $k_0 = 2\pi, \theta^{inc} = \pi/2$.

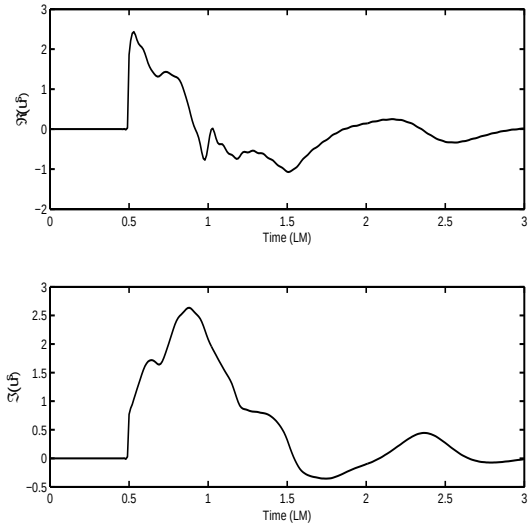

Figure 6: Change history of scattered field for TE polarization at $r = 0.3m, \theta = \pi/2$ with $k_0 = 2\pi, \theta^{inc} = \pi/2$.

5.1 Field calculations

We assume that when time $t > t_s$ and $t < t_e$, there is a incident field defined as

$$u^i = e^{x\alpha + y\beta} e^{ik_0 t}. \tag{5.4}$$

The reflected field is then

$$u^r = -e^{x\alpha - y\beta} e^{ik_0 t} \tag{5.5}$$

for TM, and

$$u^r = e^{x\alpha - y\beta} e^{ik_0 t} \tag{5.6}$$

for TE, where $\alpha = ik_0 \cos(\theta^{inc})$, $\beta = ik_0 \sin(\theta^{inc})$, θ^{inc} is incident angle, and $k_0 = 2\pi$. We observe that the incident and reflected fields are weak solutions of Equation (3.1).

The scattered fields at two selected (interior) nodes are plotted in Figs. 5 and 6 for TM and TE polarizations respectively. The exterior solutions are solved using Equation (3.9) for the TM polarization and Equation (4.5) for TE.

Figs. 7 and 8 depict the scattered fields throughout the entire domain. The perfect link between the approximated (interior) solution and the exact (exterior) solution indicates the reliability of the method.

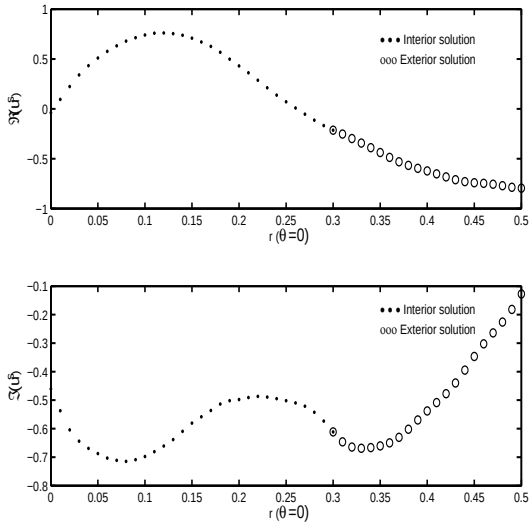

Figure 7: Link of scattered field for TM polarization at $r = 0.3m, \theta = \pi/2$ with $k_0 = 2\pi, \theta^{inc} = \pi/2$.

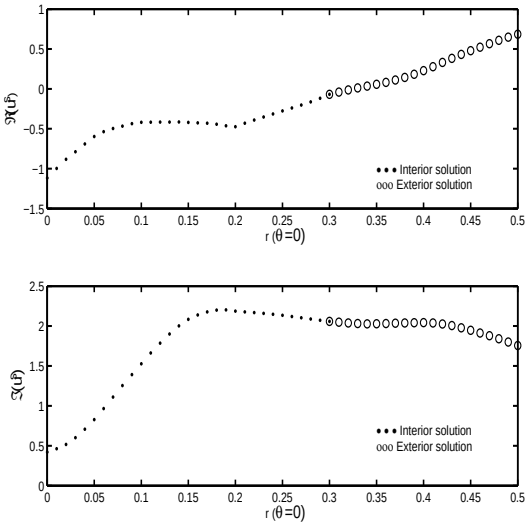

Figure 8: Link of scattered field for TE polarization at $r = 0.3m, \theta = \pi/2$ with $k_0 = 2\pi, \theta^{inc} = \pi/2$.

5.2 Convergence analysis

The convergence rates of the method are examined for both polarizations using the round cavity geometry. The relative errors in the L^2-norm and the H^1-norm are defined as:

$$\mathbf{error}_n = \begin{cases} \log_2 \dfrac{\|u_{A_n^e} - u_{A_{n-1}^e}\|_0}{\|u_{A_n^e}\|_0} & \text{for } L^2\text{-norm}, \\ \log_2 \dfrac{\|u_{A_n^e} - u_{A_{n-1}^e}\|_1}{\|u_{A_n^e}\|_1} & \text{for } H^1\text{-norm}, \end{cases}$$

where A_n^e is the average element area at the n^{th} mesh refinement. The relative errors are plotted against the reciprocal of the average element area $1/A_n^e$ in Fig. 9 for the TM case. As indicated in [20], the error in the H^1-norm is of order $\mathcal{O}(h)$, versus $\mathcal{O}(h^2)$ of the L^2-norm, where h is the element dimension.

6 Conclusion

We have implemented a finite element/Fourier transform method for the time domain scattering of plane waves by overfilled cavities embedded in the 2D ground plane. The reliability of the method is demonstrated by the perfect linkage between the numerical solutions of the interior problem and those of the analytical over the exterior. Finally the convergence charts confirm the error analysis in [20], which is helpful in determining the mesh refinement for specified error tolerance.

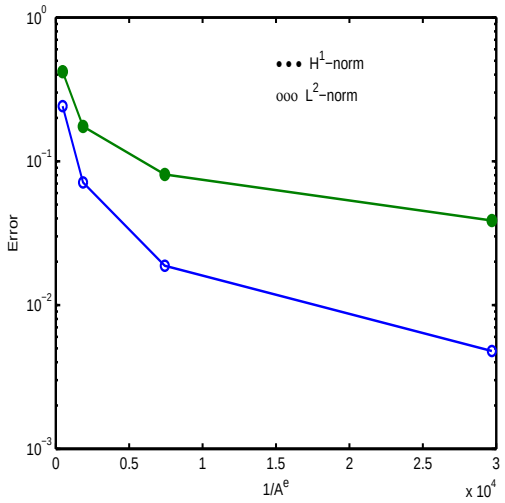

Figure 9: Relative error versus the reciprocal of average element area for TM polarization, $k_0 = 2\pi, \theta^{inc} = \pi/2$.

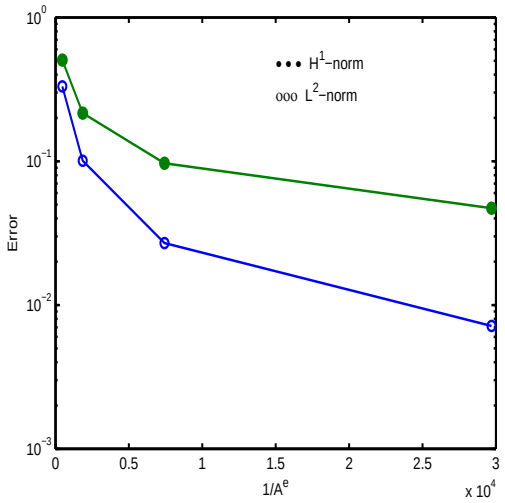

Figure 10: Relative error versus the reciprocal of average element area for TE polarization, $k_0 = 2\pi, \theta^{inc} = \pi/2$.

Acknowledgments

The views expressed in this article are those of the authors and do not reflect the official policy or position of the United States Air Force, Department of Defense, or the US Government.

References

[1] T. Abboud and T. Sayah, Potentiels retardés pour les obstacles homogènes par morceaux, Rapport interne au CMAP, no. 390, École Polytechnique 1998.
[2] H. Ammari, G. Bao and A. Wood, An integral equation method for the electromagnetic scattering from cavities, Math. Meth. Appl. Sci., 23 (2000), 1057–1072.
[3] H. Ammari, G. Bao and A. Wood, Analysis of the electromagnetic scattering from a cavity, Japan J. Indus. Appl. Math., 19(2) (2001), 301–308.
[4] H. Ammari, G. Bao and A. Wood, A cavity problem for Maxwell's equations, Meth. Math. Appl., 9(2) (2002), 249–260.
[5] R. J. Burkholder, Two ray shooting methods for computing the em scattering by large open-ended cavities, Comput. Phys. Commun., 68(1-3) (1991), 353–65.
[6] R. L. Clary, Ram2d: Two Dimensional Integral Equation Computer Code, Version 3.0, Northrop Grumman Cor., 1995.
[7] D. Givoli, Non reflecting boundary conditions, J. Comput. Phys., 94 (1991), 1–29.
[8] T. B. Hansen and A. D. Yaghjian, Low-frequency scattering from two-dimensional perfect conductors, IEEE T. Antennas. Propag., 40(11) (1992), 1389–1402.
[9] J. M. Jin, Electromagnetic scattering from large, deep, and arbitrarily-shaped open cavities, Electromagnetics, 18(1) (1998), 3–34.
[10] J. M. Jin, S. Ni and S. W. Lee, Hybridization of sbr and fem for scattering by large bodies with cracks and cavities, IEEE T. Antennas. Propag., 43 (1995), 1130–1139.

[11] J. M. Jin and J. L. Volakis, A hybrid finite element method for scattering and radiation by microstrip patch antennas and arrays residing in a cavity, IEEE T. Antennas. Propag., 39 (1991), 1598–1604.
[12] H. Ling, R. C. Chou and S. W. Lee, Shooting and bouncing rays: Calculating the rcs of an arbitrarily shaped cavity, IEEE T. Antenns. Propag., 37(2) (1989), 194–205.
[13] J. Liu and J. M. Jin, A special higher order finite-element method for scattering by deep cavities, IEEE T. Antennas. Propag., 48 (2000), 694–703.
[14] D. H. Reuster and G. A. Thiele, A field iterative method for computing the scattered electric fields at the apertures of large perfectly conducting cavities, IEEE T. Antennas. Propag., 43(3) (1995), 286–290.
[15] T. Van and A. Wood, Analysis of time-domain Maxwell's equations for 3-D cavities, Adv. Comput. Math., 16 (2002), 211–228.
[16] T. Van and A. Wood, Finite element analysis for 2-D cavity problem, IEEE T. Antennas. Propag., 51(1) (2003), 1–8.
[17] T. Van and A. Wood, A time-marching finite element method for an electromagnetic scattering problem, Math. Meth. Appl. Sci., 26 (2003), 1025–145.
[18] T. Van and A. Wood, Analysis of transient electromagnetic scattering from over-filled cavities, SIAM J. Appl. Math. 64 (2004), 688–708.
[19] T. M. Wang and H. Ling, Electromagnetic scattering from three-dimensional cavities via a connection scheme, IEEE T. Antennas. Propag., 39 (1991), 1505–1513.
[20] A. W. Wood, Analysis of electromagnetic scattering from an over-filled cavity in the ground plane, J. Comput. Phys., to appear.
[21] W. D. Wood and A. W. Wood, Development and numerical solution of integral equations for electromagnetic scattering from a trough in a ground plane, IEEE T. Antennas. Propag., 47(8) (1999), 1318–1322.